ELSEVIER

Coordination Chemistry Reviews 229 (2002) 9–16

COORDINATION CHEMISTRY REVIEWS

www.elsevier.com/locate/ccr

Ground- and excited-state reactivities of cationic sandwich and half-sandwich complexes of iron(II)

Cheryl A. Turner, Wei Ding, I. Jonathan Amster, Charles Kutal *

Department of Chemistry, University of Georgia, Athens, GA 30602 2556, USA

Received 29 October 2001; accepted 21 December 2001

Contents

Abstract

Irradiation of cationic complexes belonging to the $[CpFe(\eta^6\text{-arene})]^+$ family (Cp is $\eta^5\text{-}C_5H_5$) results in the substitution of arene by solvent or other potential ligands present in solution. In solutions containing an epoxide monomer, this photochemical reaction generates a species that initiates polymerization. While several studies of this commercially important process have been reported, the nature of the active initiating species has remained largely conjectural. We have undertaken an investigation that employs two powerful techniques—ion cyclotron resonance Fourier transform mass spectrometry and electrospray ionization mass spectrometry—to elucidate the mechanism of photoinitiated polymerization in systems containing $[CpFe(\eta^6\text{-arene})]^+$ complexes. These techniques have led to the first direct observation of several cationic photoproducts that can serve as initiators for epoxide polymerization. Our results and their mechanistic implications form the subjects of this article.

Keywords: Fourier transform mass spectrometry; Cationic complexes; Photochemical reactions; Electrospray ionization mass spectrometry

1. Introduction

Cationic metal-sandwich complexes of general formula $[CpFe(\eta^6\text{-arene})]^+$ (Cp is $\eta^5\text{-}C_5H_5$) have been the subject of several photochemical investigations [1–8]. Irradiation of these low-spin, d^6 systems in the region of their ligand field absorption bands induces loss of arene to produce $[CpFe(L)_3]^+$ (Eq. (1)), where L can be solvent or any potential ligand present in solution. When L is weakly coordinating, the half-sandwich complex is unstable and decomposes in a secondary thermal reaction (Eq. (2)). Commercial interest in members of the $[CpFe(\eta^6\text{-arene})]^+$ family arises from their use as visible-light sensitive

$$[CpFe(\eta^6\text{arene})]^+ \xrightarrow[L]{h\nu} [CpFe(L)_3]^+ + \text{arene} \quad (1)$$

$$2[CpFe(L)_3]^+ \rightarrow [Fe(L)_6]^{2+} + FeCp_2 \quad (2)$$

* Corresponding author. Tel.: +1-706-542-2035; fax: +1-706-542-9454

E-mail address: ckutal@sunchem.chem.uga.edu (C. Kutal).

0010-8545/02/$ - see front matter
PII: S0010-8545(02)00109-1

photoinitiators for the polymerizations of an assortment of monomers, including epoxides [9–13], dicyanate esters [14], pyrrole [15], and acrylates [16,17]. Despite several studies of these systems, the identity of the photogenerated species actually responsible for initiating the polymerization process remains the subject of considerable conjecture. The conventional mechanism [9–13] assigns this role to $[CpFe(monomer)_3]^+$ (Eq. (3), illustrated for an epoxide monomer), but neither it nor any polymeric products containing the $[FeCp]^+$ fragment have been observed. Accordingly, we have undertaken a comprehensive investigation designed to (i) explore the reactivity of $[FeCp]^+$ with a variety of substrates, (ii) assess the role of $[FeCp]^+$ and its complexes (e.g. $[CpFe(monomer)_3]^+$) in initiating polymerization reactions, (iii) identify other possible initiating species formed upon irradiating $[CpFe(\eta^6\text{-arene})]^+$ in the presence of a monomer, and (iv) monitor the first few steps in the polymerization process.

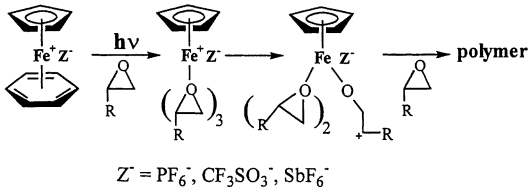

(3)

Two mass spectrometric techniques have proven to be particularly valuable in our work. The first, Fourier transform ion cyclotron resonance mass spectrometry (FTICR-MS) has been used to trap $[FeCp]^+$ in the gas phase and monitor its reactions with added substrates without interference from solvent. We have found that this highly coordinatively-unsaturated (12 valence electrons) iron(II) complex undergoes a rich chemistry that includes atom abstraction, substrate coordination, and electron transfer. Particularly interesting is the observation that the relative importance of these pathways depends upon the internal energy content of $[FeCp]^+$. The second technique, electrospray ionization mass spectrometry (ESI-MS), has been used for the on-line identification of cationic species generated during the solution photolysis of $[CpFe(\eta^6\text{-arene})]^+$. Several of these species, including one that contains no iron, have been found to initiate the polymerization of an epoxide. Consequently, the conventional mechanism of photoinitiated polymerization involving only $[CpFe(monomer)_3]^+$ intermediates (Eq. (3)) must be modified to accommodate these results. Succeeding sections of this article will provide more detailed descriptions of our FTICR-MS and ESI-MS experiments, and illustrate the power of these mass spectrometric techniques in providing important and, in some cases, previously unobtainable mechanistic information.

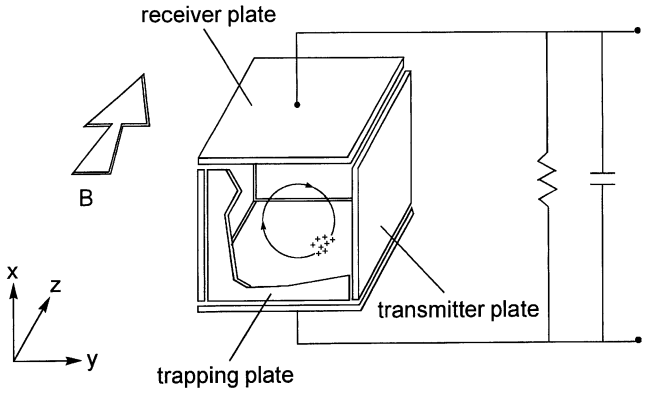

Fig. 1. Schematic diagram of a trapped ion cell used in the FTICR-MS experiments. Vector B defines the direction of the magnetic field lines.

2. Studies of $CpFe^+$ in the gas phase

2.1. Description of the FTICR-MS technique

Comprehensive accounts of the theory, instrumentation, and applications of FTICR-MS can be found in several reviews [18–21]. For this discussion, it will suffice to summarize the general features of the technique and, as appropriate, provide specific examples from our work.

The key events in an FTICR-MS experiment occur in a trapped ion cell of the type depicted in Fig. 1. In our studies, the cell was operated exclusively in the positive ion mode. Three sets of parallel plates, which are labeled according to their function, serve as the cell walls. The cell is enclosed within a high vacuum chamber and centered in a homogeneous magnetic field. Under the influence of this field, cationic species in the cell move in circular orbits that lie perpendicular to the field direction. This cyclotron motion occurs with a frequency (ν_c) that depends upon the charge/mass ratio (q/m) of an ion and the field strength (B, Eq. (4)). Leakage of ions out of the cell along the direction of the magnetic field (z axis) is prevented by a small positive voltage applied to the trapping plates. At this point in the experiment, the ensemble of trapped ions undergoes random (non-coherent) cyclotron motion, and no signal can be detected. Applying a short duration, high intensity radio frequency signal to the transmitter plates excites the ions into larger orbits and causes them to move as a coherent packet. The orbiting packet of positive charge induces an image current, which is detected by the receiver plates. This signal, which contains contributions from ions of different q/m ratios, is converted to a voltage, amplified, digitized, and stored in a computer. The resulting time domain spectrum is Fourier transformed to a frequency domain spectrum, and then converted to the familiar mass spectrum format using the relationship

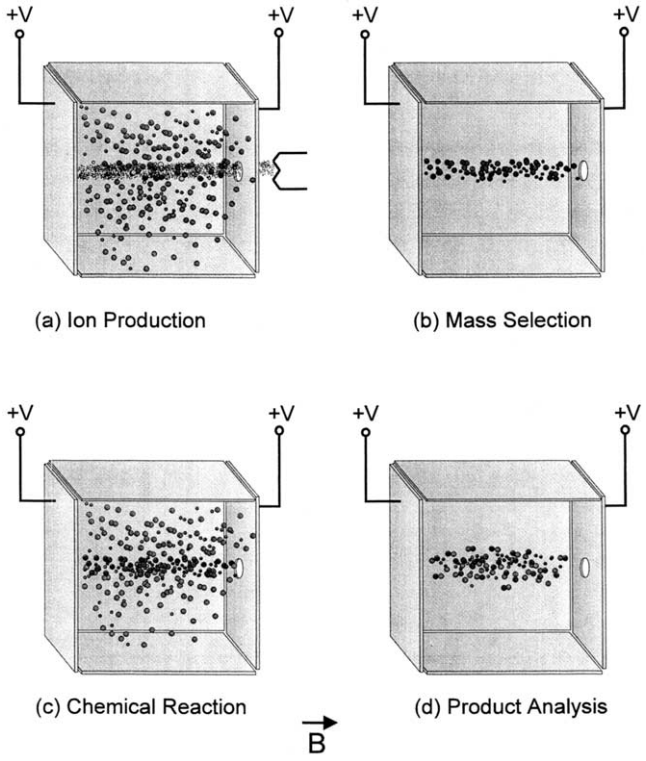

Fig. 2. Sequential steps in a typical FTICR-MS experiment: (a) electron beam dissociative ionization of an uncharged precursor (e.g. $FeCp_2$), (b) mass selection of ion of interest, (c) reaction of mass selected ion with an uncharged reagent, (d) mass analysis of reaction products.

in Eq. (4).

$$v_c = \frac{qB}{2\pi m} \tag{4}$$

A typical experimental sequence used in our studies is represented schematically in Fig. 2. Gaseous ferrocene ($FeCp_2$) is admitted into the ICR cell and bombarded with a beam of 70 eV electrons (step a). The ensuing dissociative ionization of the neutral reagent produces Fe^+, $[FeCp]^+$, and $[FeCp_2]^+$. An alternative route to these ions involves dissociative charge exchange of $FeCp_2$ with CO_2^+ that had been formed by electron-beam ionization of CO_2. Since we are interested in the chemistry of $[FeCp]^+$, it is convenient to remove all other ions from the cell prior to admitting potential reactants. This task is accomplished with a process termed double resonance, in which a high power pulse at the cyclotron frequencies of Fe^+ and $[FeCp_2]^+$ excites these species to sufficiently large orbits that they are neutralized on the cell walls (step b). Thereafter, $[FeCp]^+$ is reacted with an added reagent gas (step c). In some experiments, the internal energy of nascent $[FeCp]^+$ is varied in a systematic manner by collisional cooling with a buffer gas prior to adding the reagent. During this cooling process, the ions are held at the middle of the cell by quadrupolar excitation [22,23]. Finally, all ionic products are mass analyzed by the techniques already described (step d).

2.2. Reactivity of $[FeCp]^+$ in the gas phase

Reaction of $[FeCp]^+$ with ethylene oxide yields $[CpFeO]^+$ and $[CpFeO_2]^+$ as the major metal-containing products (Eq. (5)) [24,25]. Since molecular adducts of the type $[CpFe(epoxide)_3]^+$ are not observed down to the shortest detection time ($\sim$50 ms) of our instrument coordinated epoxide must undergo rapid ring fragmentation accompanied by elimination of ethylene. We have proposed that ring opening initially produces a metallocyclobutane intermediate, which then undergoes olefin loss through cleavage of Fe–C and O–C bonds (Eq. (6)). This proposal receives support from the detection of a small amount of $[CpFeCH_2]^+$, the alternative metal-containing product expected if the metallocyclobutane eliminates formaldehyde via Fe–O and C–C bond breaking. Increasing the epoxide pressure favors formation of $[CpFeO_2]^+$ at the expense of $[CpFeO]^+$, consistent with the operation of a sequential reaction involving two epoxide molecules (Eq. (5)).

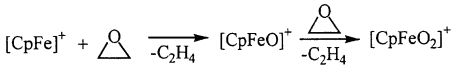

(5)

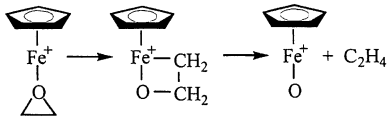

(6)

Ring-opening atom abstraction also occurs upon reacting ethylene sulfide with $[FeCp]^+$ (substitute S for O in Eq. (5)). Such metal-assisted fragmentation of three-membered heterocycles is facilitated by the resulting relief of ring strain and the direct elimination of the stable neutral molecule, ethylene. Consistent with this explanation, we find that up to two molecules of trimethylene oxide (TMO) or tetrahydrofuran (THF) coordinate to $[FeCp]^+$ (Eq. (7)) with little ring fragmentation. THF is less strained than ethylene oxide, and neither it nor TMO could directly produce a stable neutral following oxygen atom loss. Electron transfer from an uncharged substrate to $[FeCp]^+$ constitutes a third reaction channel. For ethylene oxide, this redox process initially generates the $C_2H_4O^{+\bullet}$ radical cation (Eq. (8)), which, in a rapid follow up step, abstracts a hydrogen atom from a neutral epoxide molecule to yield the predominant product, $C_2H_5O^{+\bullet}$ (Eq. (9)).

$$[CpFe]^+ \underset{THF}{\rightarrow} [CpFe(THF)]^+ \underset{THF}{\rightarrow} [CpFe(THF)_2]^+ \quad (7)$$

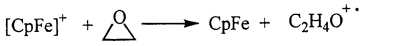

$$[CpFe]^+ + \text{epoxide} \longrightarrow CpFe + C_2H_4O^{+\cdot} \quad (8)$$

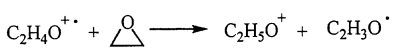

$$C_2H_4O^{+\cdot} + \text{epoxide} \longrightarrow C_2H_5O^+ + C_2H_3O^{\cdot} \quad (9)$$

Electron transfer to $[FeCp]^+$ also occurs with several other uncharged substrates: ferrocene, naphthalene, anisole, mesitylene, ethylene sulfide, THF, and TMO [26]. For $[FeCp]^+$ in its electronic ground state, the enthalpy of this process is governed by the relationship in Eq. (10), where EA($[FeCp]^+$) is the electron affinity of the iron complex and IE(M) is the ionization energy of the substrate. A straightforward thermochemical calculation yields EA($[FeCp]^+$) = 6.7 eV, while measured values of IE(M) range from 6.99 to 10.57 eV for the group of substrates listed above. Substitution of these data into Eq. (10) leads to the conclusion that electron transfer to the electronic ground state of $[FeCp]^+$ is energetically unfavorable ($\Delta H > 0$) for every substrate examined. That this reaction does occur requires $[FeCp]^+$ to possess considerable excess internal energy. For example, electron transfer from ethylene oxide to ground state $[FeCp]^+$ is endothermic by 3.9 eV; accordingly, the metal complex must contain at least this amount of excess energy for reaction to occur. Since vibrational–rotational excitation of this magnitude appears unlikely, we conclude that electron transfer originates from one or more electronically excited state(s) of $[FeCp]^+$.

$$\Delta H = \text{IE(M)} - \text{EA}([CpFe]^+) \quad (10)$$

The energetics of atom abstraction (Eq. (5)) and substrate coordination (Eq. (7)) are less certain. An approximate calculation indicates that $\Delta H < 0$ for the abstraction of the oxygen atom from ethylene oxide by $[FeCp]^+$. Likewise, coordination of a Lewis base such as ethylene oxide or THF to the electron deficient metal center should be exothermic. It appears reasonable, therefore, to expect that both processes can occur in the electronic ground state of $[FeCp]^+$.

The relationship between the internal energy of $[FeCp]^+$ and its chemical reactivity was investigated in a series of experiments that employed collisional cooling [26]. This technique allows systematic variations to be made in the average internal energy of the ions prior to their reaction with added substrate. In one set of experiments, we examined the electron transfer reaction between $[FeCp]^+$ and $FeCp_2$ (Eq. (11)). This process, which is slightly endothermic ($\Delta H \sim 0.3$ eV) when both reactants reside in their electronic ground states, provides a sensitive measure of the internal energy content of $[FeCp]^+$. For $[FeCp]^+$ that had not undergone collisional cooling, reaction with excess $FeCp_2$ pulsed into the ICR cell was nearly complete within a time frame of 150 ms (Fig. 3). Moreover, disappearance of the reactant ion followed non-exponential kinetics. In contrast, $[FeCp]^+$ that had undergone 1800 collisions with CO_2 exhibited sharply reduced reactivity toward $FeCp_2$ and a more exponential decay plot (Fig. 4). Minimally, these results establish that electron transfer (Eq. (11)) is sensitive to the internal energy of $[FeCp]^+$ [27]. In addition, they support our earlier conclusion that this endothermic reaction originates from one or more electronic excited state(s) of the ion.

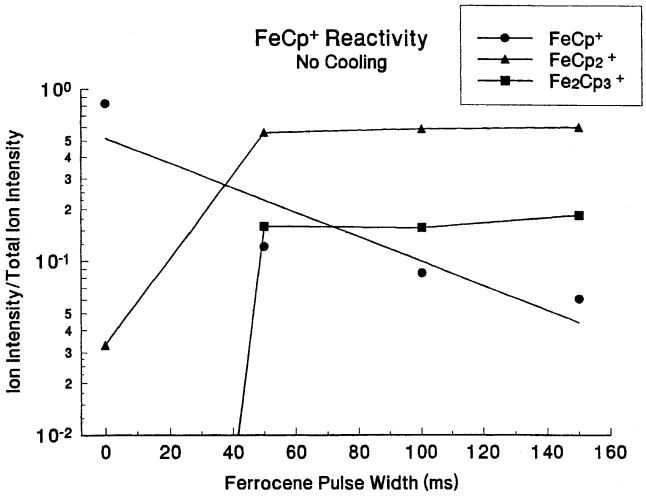

Fig. 3. Abundances of reactant and product ions for the charge transfer reaction between uncooled $[FeCp]^+$ and $FeCp_2$ (note: $[Fe_2Cp_3]^+$ results from a secondary reaction of $[FeCp_2]^+$ and $FeCp_2$). The abscissa is plotted as the duration of the pulse that admits gaseous $FeCp_2$ into the ICR cell, and is proportional to the number of collisions between the reactants.

$$[CpFe]^+ + FeCp_2 \rightarrow CpFe + [FeCp_2]^+ \quad (11)$$

In a second set of experiments involving collisional cooling, we investigated the internal energy dependence

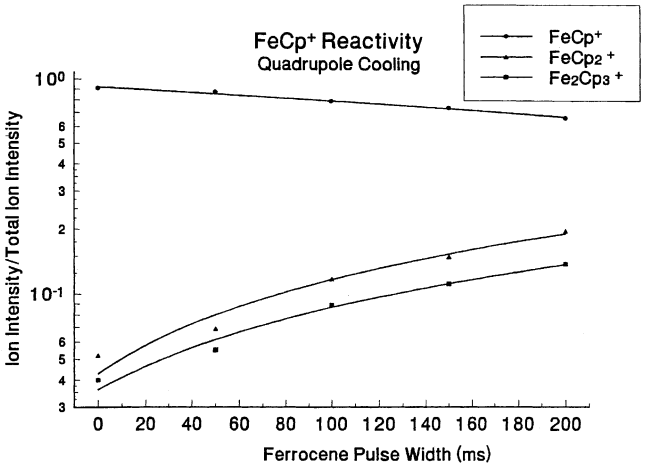

Fig. 4. Abundances of reactant and product ions for the charge transfer reaction between collisionally-cooled $[FeCp]^+$ and $FeCp_2$. Refer to Fig. 3 caption for other details.

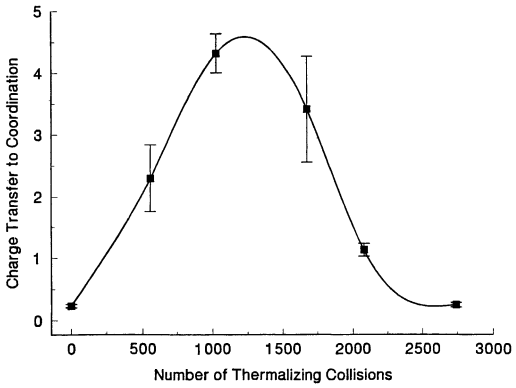

Fig. 5. Ratio of electron transfer to substrate coordination in the $[FeCp]^+$/THF system vs. the number of cooling collisions undergone by $[FeCp]^+$.

of the reactions of $[FeCp]^+$ with THF [26]. Fig. 5 reveals that the relative importance of the two reaction channels, electron transfer and coordination (Eq. (7)), varies with the number of thermalizing collisions. Coordination of THF dominates when the internal energy of $[FeCp]^+$ is high (few collisions) or low (numerous collisions), whereas electron transfer is favored at intermediate energy contents. The behavior observed in the low internal-energy regime reflects the reactivity of the electronic ground state of $[FeCp]^+$. With little excess energy, this state favors exothermic coordination over endothermic electron transfer. The greater importance of electron transfer with increasing internal energy is consistent with a growing fraction of $[FeCp]^+$ reacting from an electronic excited state that lies at least 2.7 eV above the ground state. Electron transfer from THF to the excited metal complex is energetically favorable ($\Delta H < 0$) and, evidently, the preferred pathway. Further increases in the internal energy of $[FeCp]^+$ eventually results in a decline in the importance of electron transfer relative to coordination. This intriguing behavior could result from the population of a second, higher lying electronic excited state of $[FeCp]^+$ that undergoes exothermic electron transfer with THF. Conceivably, ΔH becomes so negative for this process that it occurs in the Marcus inverted region with a greatly reduced rate constant [28]. Further examination of the behavior in the high internal energy regime is needed to test this possibility.

While caution must be exercised in extrapolating gas phase reactivity data to the condensed phase, it is instructive to consider our FTICR-MS results within the context of the conventional mechanism of photoinitiated epoxide polymerization (Eq. (3)). Clearly, the reactivity of $[FeCp]^+$ confirms the ability of this iron-containing fragment to cleave the C–O bond of a coordinated epoxide molecule. In the gas phase the loss of ethylene from a metallocyclobutane intermediate (Eq. (6)) occurs rapidly compared with the mean time between collisions (10–100 ms) with additional epoxide molecules and, as a consequence, the oxygen atom-transfer products, $[CpFeO]^+$ and $[CpFeO_2]^+$, are obtained. In contrast, the greater collision frequency in condensed media enhances the likelihood that coordinated epoxide in species such as $[CpFe(epoxide)_3]^+$ will undergo ring opening and addition of another epoxide molecule, thereby initiating polymerization. We turn now to our ESI-MS studies for further information about the initiation process.

3. Studies of $CpFe(\eta^6\text{-arene})^+$ in solution

3.1. Description of the ESI-MS technique

ESI-MS is a soft ionization technique that allows the transfer of ions from solution to the gas phase with little fragmentation, thus simplifying interpretation of the mass spectrum [29–33]. ESI-MS also offers the possibility of trapping and identifying short-lived intermediates, since bimolecular processes involving ionic species in solution are greatly attenuated when the ions pass into the gas phase [34–38]. These characteristics make the technique well suited for mechanistic studies of photoinitiated cationic polymerization involving $[CpFe(\eta^6\text{-arene})]^+$ complexes.

Our ESI-MS experiments were performed in the positive ion mode on a PerSeptive Biosystems Mariner Workstation, an apparatus that combines a time-of-flight mass spectrometer with an electrospray source. A schematic diagram of this apparatus and the other components used for on-line photochemical studies are shown in Fig. 6. An optically transparent nanospray tip

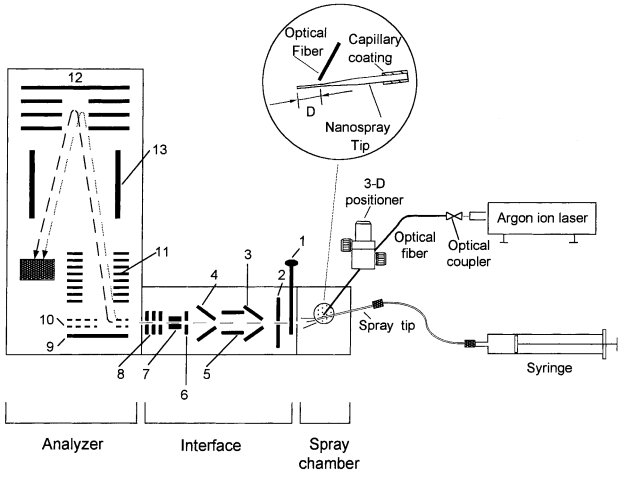

Fig. 6. Schematic diagram of the ESI-MS apparatus used for on-line photochemical experiments. Numbered components are identified as follows: (1) shutter, (2) nozzle, (3) skimmer 1, (4) skimmer 2, (5) quadrupole, (6) extraction lens, (7) deflector, (8) Einzel lens, (9) push electrode, (10) pull electrode, (11) accelerating lens stack, (12) reflector, (13) flight tube.

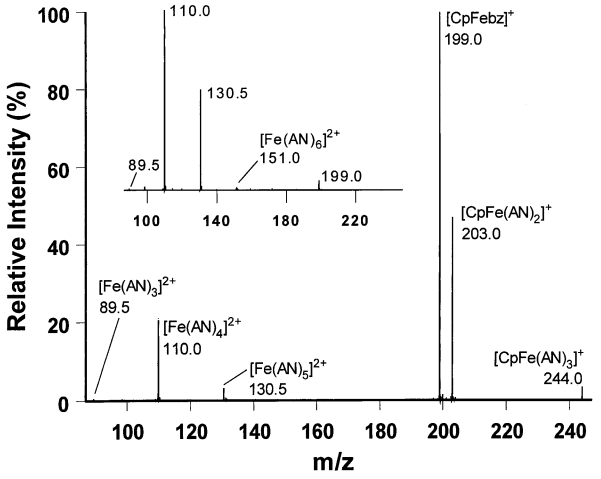

Fig. 7. Electrospray ionization mass spectrum of photolysis products from a 70 μM solution of $[CpFebz]^+$ in AN with $D = 1.2$ mm. Inset: spectrum of same sample with $D = 4$ mm.

was fabricated from fused silica tubing (100 μm i.d.). The tip was drawn to a fine point (10–20 μm i.d.) at the spray-delivery end, and connected at the other end to a syringe pump. Solutions containing $[CpFebz]PF_6$ (bz is η^6-benzene) were irradiated directly in the tip by an optical fiber that delivered 488 nm light from an argon ion laser. Since the same photoproducts were obtained over a range of laser powers, multiphoton excitation and secondary photolysis processes were unimportant. The distance, D, between the midpoint of the irradiated zone and the tip end, could be varied by adjusting the position of the fiber with a precision translation stage. With $D = 1.7$ mm and flow rates of 20–80 μl h^{-1}, photoproducts required < 100 ms to arrive at the tip end for spraying.

3.2. Reactivity of $[CpFe(\eta^6\text{-arene})]^+$ in solution

Control experiments confirmed that $[CpFebz]^+$ emerged unchanged from the nanospray tip in the absence of light. Irradiation of an acetonitrile (AN) solution of the complex in the tip generated two major series of ionic products: $[CpFe(AN)_{1-3}]^+$ and $[Fe(AN)_{3-6}]^{2+}$ (Fig. 7) [39]. The first series reflects the photodissociation of benzene (Eq. (1)), while the second series arises from the subsequent thermal loss of the cyclopentadienide anion (Eq. (2)). The coordinatively-unsaturated species observed within each series (e.g. five-coordinate $[CpFe(AN)_2]^+$ and four-coordinate $[Fe(AN)_4]^{2+}$) resulted from collisionally-induced dissociation of AN from $[CpFe(AN)_3]^+$ and $[Fe(AN)_6]^{2+}$ in the region following the first skimmer. Consistent with this explanation, we observed that increasing the kinetic energy of the electrosprayed ions by raising the skimmer voltage favored the production of species with fewer coordinated AN molecules. The parent–offspring relationship between $[CpFe(AN)_3]^+$ and $[Fe(AN)_6]^{2+}$ is evident from the dependence of the product distribution on D (inset to Fig. 7). Increasing D at a constant flow rate lengthens the time that $[CpFe(AN)_3]^+$ spends in solution before exiting the spray tip. Consequently, thermal decomposition of this primary photoproduct to $[Fe(AN)_6]^{2+}$ (Eq. (2)) becomes increasingly important and results in a greater abundance of solvated Fe^{2+} species.

Photolysis of $[CpFebz]^+$ in AN solutions containing cyclohexene oxide (CHO) yielded the same products observed in pure AN, as well as a few new species. Using a high CHO concentration (0.4 M), we detected $[Fe(AN)_3(CHO)]^{2+}$ and $[Fe(AN)_4(CHO)]^{2+}$, but found no products containing more than one epoxide molecule. The latter result indicates that the poorly coordinating CHO does not compete effectively with AN for binding sites about Fe(II). Another product, X^+ ($m/z = 140$), has not yet been identified, but an analysis of isotope patterns has established that it does not contain iron. At high CHO concentrations, a species corresponding to $[X(CHO)]^+$ was detected.

Irradiating $[CpFebz]^+$ and CHO in the weakly coordinating solvent, 1,2-dichloroethane (DCE), yielded a rich assortment of new products. With $D = 8$ mm, series corresponding to $[(H_2O)Fe(CHO)_{4-12}]^{2+}$, $[Fe(CHO)_{5-8}]^{2+}$, and $[X(CHO)_{0-5}]^+$ were detected (Fig. 8). The water present in the Fe-containing products most likely originated from traces of moisture introduced to the rigorously dried solvent during sample preparation and/or present in the ambient atmosphere at the electrospray tip exit. Additional series, $[(H_2O)CpFe(CHO)_{1-4}]^+$ and $[CpFe(CHO)_{1-5}]^+$ (inset to Fig. 8), appeared with $D \leq 0.5$ mm. This behavior indicates that the latter two series possess short lifetimes

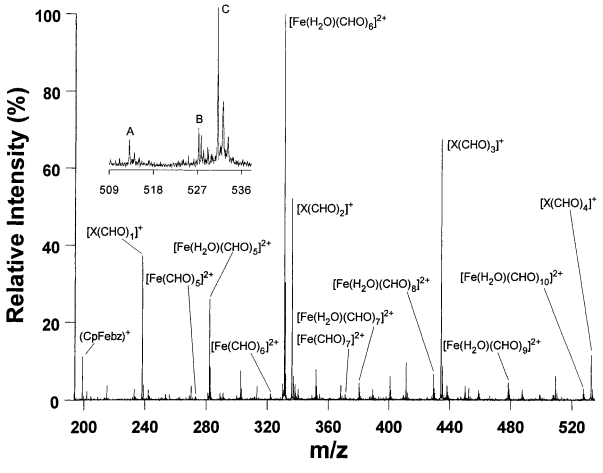

Fig. 8. Electrospray ionization mass spectrum of photolysis products from a DCE solution containing 41 μM $[CpFebz]^+$ and 40 mM cyclohexene oxide (CHO) with $D = 8$ mm. Inset: representative members of three product series observed with $D \sim 0.5$ mm: A, $[CpFe(CHO)_4]^+$; B, $[(H_2O)Fe(CHO)_{10}]^{2+}$; C, $[(H_2O)CpFe(CHO)_4]^+$.

(<50 ms) in solution and only can be observed when generated near the tip end. Recall that a similar situation exists for $[CpFe(AN)_3]^+$.

It is unlikely that all of the molecules present in the heavier Fe-containing products (e.g. $[(H_2O)Fe(CHO)_{12}]^{2+}$, $[Fe(CHO)_8]^{2+}$ and $[CpFe(CHO)_5]^+$) are bound directly to the metal, since dipositive iron rarely exhibits coordination numbers above 6 [40]. Instead, we have proposed a model in which the metal can accommodate up to six CHO molecules in its first coordination sphere. Binding to the cationic metal renders the epoxide susceptible to nucleophilic attack by the oxygen atom of an uncoordinated monomer unit (Eq. (12)) [41]. The ensuing C–O bond formation opens the strained three-membered ring and creates another cationic site for continued chain growth. According to this model, which accommodates all of our experimental observations, products such as $[(H_2O)Fe(CHO)_{12}]^{2+}$, $[Fe(CHO)_8]^{2+}$ and $[CpFe(CHO)_5]^+$ contain a growing polymer chain bound directly to the metal center. In essence, the ESI-MS technique has allowed us to observe the first few steps in the polymerization of an epoxide initiated by cationic iron species. The observation that X^+ forms products containing up to five CHO units also is consistent with the polymer model, and we have proposed that this non-iron species also is an active initiator for epoxide polymerization.

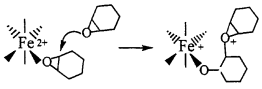

(12)

4. Concluding remarks

The studies reported here have provided several new insights concerning the reactivity of $[FeCp]^+$ and its complexes of the type $[CpFe(\eta^6\text{-arene})]^+$. Using the technique of FTICR-MS, we have demonstrated that the highly coordinatively-unsaturated $[FeCp]^+$ cation undergoes a rich chemistry with uncharged substrates in the gas phase. Atom transfer and substrate coordination pathways proceed via the electronic ground state of the cation, while electron transfer involves one or more excited state(s). Consequently, the relative importance of these pathways depends upon the internal energy content of $[FeCp]^+$. Collisional cooling experiments have revealed that a surprisingly large number (>1000) of collisions are required to relax the electronically-excited cation to its ground state.

Irradiating monomer-containing solutions of $[CpFe(\eta^6\text{-arene})]^+$ in the tip of an electrospray ionization source and analyzing the photoproducts by mass spectrometry holds considerable promise for probing the mechanism by which these complexes serve as photoinitiators for cationic polymerization. For the specific example of $[CpFebz]^+$ in epoxide-containing solutions, this ESI-MS technique has provided the first direct support for earlier proposals that photogenerated $[CpFe(epoxide)_3]^+$ is involved in initiating polymerization. Moreover, at least two other initiating species have been identified: Fe^{2+} complexes that result from the thermal decomposition of $[CpFe(epoxide)_3]^+$, and a non-iron containing species, X^+. Consequently, the roles of several cationic species should be considered in future mechanistic discussions of photoinitiated polymerization involving $[CpFe(\eta^6\text{-arene})]^+$ complexes.[34].

Acknowledgements

The authors are grateful to Dr. Bentley J. Palmer and Dr. Keith A. Johnson for their contributions to this work. We thank the National Science Foundation (Grants DMR-9122653 and CHE-9974579) and the University of Georgia Research Foundation for financial support.

References

[1] T.P. Gill, K.R. Mann, Inorg. Chem. 22 (1983) 1986.
[2] J.L. Schrenk, M.C. Palazzotto, K.R. Mann, Inorg. Chem. 22 (1983) 4047.
[3] A.M. McNair, J.L. Schrenk, K.R. Mann, Inorg. Chem. 23 (1984) 2633.
[4] E. Roman, M. Barrera, S. Hernandez, E. Lissi, J. Chem. Soc. Perkin Trans. II (1988) 939.
[5] S. Ronco, G. Ferraudi, E. Roman, S. Hernandez, Inorg. Chim. Acta 161 (1989) 183.
[6] D.R. Chrisope, K.M. Park, G.B. Schuster, J. Am. Chem. Soc. 111 (1989) 195.
[7] T. Karatsu, Y. Shibuki, N. Miyagawa, S. Takahara, A. Kitamura, T. Yamaoka, J. Photochem. Photobiol. A: Chem. 107 (1997) 83.
[8] V. Jabubek, A.J. Lees, Inorg. Chem. 39 (2000) 5779.
[9] A. Roloff, K. Meier, M. Riedeker, Pure Appl. Chem. 58 (1986) 1267.
[10] F. Lohse, H. Zweifel, Adv. Polym. Sci. 78 (1986) 61.
[11] B. Klingert, M. Riedeker, A. Roloff, Comments Inorg. Chem. 7 (1988) 109.
[12] K.M. Park, G.B. Schuster, J. Organomet. Chem. 402 (1991) 355.
[13] R. Bowser, R.S. Davidson, J. Photochem. Photobiol. A: Chem. 77 (1994) 269.
[14] T.G. Kotch, A.J. Lees, S.J. Fuerniss, K.I. Papathomas, Chem. Mater. 7 (1995) 801.
[15] J.F. Rabek, J. Lucki, M. Zuber, B.J. Qu, W.F. Shi, J. Macromol. Sci. Appl. Chem. A29 (1992) 297.
[16] P. Wang, Y. Shen, S. Wu, E. Adamczak, L. Linder, J.F. Rabek, J. Macromol. Sci. Pure Appl. Chem. A32 (1995) 1973.
[17] N.S. Allen, M. Edge, A.R. Jasso, T. Corrales, M. Tellez-Rosas, J. Photochem. Photobiol. A: Chem. 102 (1997) 253.
[18] M.L. Gross, D.L. Rempel, Science 226 (1984) 261.
[19] M.V. Buchanan, M.B. Comisarow, in: M.V. Buchanan (Ed.), Fourier Transform Mass Spectrometry: Evolution, Innovation,

and Applications (Chapter 1), American Chemical Society, Washington, DC, 1987.
[20] A.G. Marshall, L. Schweikhard, Int. J. Mass. Spectrom. Ion. Processes 118/119 (1992) 37.
[21] I.J. Amster, J. Mass Spectrom. 31 (1996) 1325.
[22] G. Savard, S. Becker, G. Bollen, H. -J. Kluge, R.B. Moore, L. Schweikhard, H. Stolzenberg, U. Wiess, Phys. Lett. A 158 (1991) 247.
[23] L. Schweikhard, S. Guan, A.G. Marshall, Int. J. Mass Spectrom. Ion. Processes 120 (1992) 71.
[24] W.J. Gwathney, L. Lin, C. Kutal, I.J. Amster, Org. Mass Spectrom. 27 (1992) 840.
[25] C. Kutal, I.J. Amster, L. Lin, B.J. Palmer, C.A. Turner, in: G. Ondrejovic, A. Sirota (Eds.), Progress in Coordination and Organometallic Chemistry, Slovak Technical University Press, Bratislava, 1997, p. 137.
[26] C.A. Turner, Master of Science Thesis, University of Georgia, 1994.
[27] Y. Huang, B.S. Freiser, J. Am. Chem. Soc. 112 (1990) 5085.
[28] G.J. Kavarnos, Fundamentals of Photoinduced Electron Transfer (Chapter 6), VCH Publishers, New York, 1993.
[29] P. Kebarle, L. Tang, Anal. Chem. 65 (1993) 972A.
[30] G.R. Agnes, G. Horlick, Appl. Spectrosc. 48 (1994) 655.
[31] R. Bakhtiar, C.E.C.A. Hop, J. Phys. Org. Chem. 12 (1999) 511.
[32] S.A. Lorenz, E.P. Maziarz, III, T.D. Wood, Appl. Spectrosc. 53 (1999) 18A.
[33] W.J. Griffiths, A.P. Jonsson, S. Liu, D.K. Rai, Y. Wang, Biochemistry 355 (2001) 545.
[34] R. Arakawa, S. Tachiyashiki, T. Matsuo, Anal. Chem. 67 (1995) 4133.
[35] R. Arakawa, L. Jian, A. Yoshimura, K. Nozaki, T. Ohno, H. Doe, T. Matsuo, Inorg. Chem. 34 (1995) 3874.
[36] R. Arakawa, S. Mimura, G. Matsubayashi, T. Matsuo, Inorg. Chem. 35 (1996) 5725.
[37] D. Feichtinger, D.A. Plattner, P. Chen, J. Am. Chem. Soc. 120 (1998) 7125.
[38] J. Traeger, Int. J. Mass Spectrom. 200 (2000) 387.
[39] W. Ding, K.A. Johnson, I.J. Amster, C. Kutal, Inorg. Chem. 40 (2001) 6865.
[40] K.F. Purcell, J.C. Kotz, Inorganic Chemistry, Saunders, Phildelphia, 1977, p. 603.
[41] G. Odian, Principles of Polymerization, second ed. (Chapter 7), Wiley-Interscience, New York, 1981.